Chapter 6
Locally Measured Neuronal Correlates of Functional MRI Signals

Amir Shmuel and Alexander Maier

Summary

Functional brain imaging techniques, such as functional MRI (fMRI), are commonly employed to estimate local changes in neuronal activity in response to stimuli or experimental tasks. However, fMRI signals are not direct measures of neuronal activity such as spikes or dendritic potentials. Instead, fMRI is used to infer changes in neuronal activity based on local metabolic and blood-based (hemodynamic) responses via intermediary processes such as neurovascular coupling and MRI contrast. This chapter reviews current concepts on the neuronal basis of fMRI signals. Although the exact relationship between the fMRI blood oxygenation level-dependent (BOLD) signal and local neural activity remains a topic of ongoing research, there is a consensus among existing studies that graded increases in neuronal responses result in a monotonous increase in metabolic and hemodynamic activity. Many of these measurements further indicate that the relationship between local neural activity and the fMRI response is approximately linear. In line with this observation, negative BOLD responses (NBRs) have been shown to be associated with decreases in neuronal activity. Spontaneous fluctuations in fMRI signals have been shown to reflect both endogenous changes in locally measured neuronal activity and components of nonneuronal origin, such as respiration. The cortical BOLD response appears to be similarly related to the local synaptic activity that is caused by local processing and the combined ascending and descending inputs to a region, as well as to the resulting spiking output under most experimental conditions. However, in cases where synaptic and spiking activity can be dissociated, the BOLD response seems to reflect local synaptic currents more closely than the population's spike rate changes.

A. Shmuel (✉)
Montreal Neurological Institute, Departments of Neurology,
Neurosurgery and Biomedical Engineering, McGill University, Montreal, QC, Canada
e-mail: amir.shmuel@mcgill.ca

A. Maier
Department of Psychology, Vanderbilt University, Nashville, TN, USA

K. Uludağ et al. (eds.), *fMRI: From Nuclear Spins to Brain Functions,*
Biological Magnetic Resonance 30, DOI 10.1007/978-1-4899-7591-1_6

Blood Oxygenation Level-Dependent Functional Imaging Signals

The majority of functional brain imaging studies in humans rely on fMRI (Bandettini et al. 1992; Kwong et al. 1992; Ogawa et al. 1992). The most commonly used fMRI contrast is the BOLD signal (Ogawa et al. 1990). The BOLD signal is inversely proportional to the local content of deoxyhemoglobin (deoxyHb). Following increases in neuronal activity, local arterial cerebral blood flow (CBF) increases to a larger extent than does the metabolic increase in oxygen consumption (Fox and Raichle 1986; Hoge et al. 1999). The resulting drop of deoxyHb content in the local capillaries, venules, and draining veins can be monitored by tracking the changing magnitude of the BOLD signal as a function of time (Buxton et al. 2004). The interpretation of fMRI data relies heavily on inferences about how the task-invoked, metabolic, and hemodynamic responses that are captured by fMRI relate to underlying local changes in neural activity. fMRI signals are only indirect measures of neuronal activity. FMRI relies on intermediary processes such as neurovascular coupling and MR contrast. It is therefore vital to understand how metabolic and hemodynamic responses relate to the underlying neural activity in order to be able to fully utilize fMRI as an effective method to study brain function.

Extracellular Neurophysiological Signals

Excitable neurons receive input signals via their synapses at their soma and their dendrites. Excitatory and inhibitory inputs take the form of excitatory and inhibitory postsynaptic potentials (excitatory postsynaptic potentials, EPSPs; inhibitory postsynaptic potentials, IPSPs), respectively. These postsynaptic potentials can be measured directly using intracellular or patch-clamp neurophysiological recordings, which are more commonly used in studies with brain slices rather than in in vivo studies. Postsynaptic *input* potentials propagate along the neuron's dendrites towards its soma. Action potentials may get initiated at the axon hillock depending on the ratio of concurrent excitatory to inhibitory synaptic inputs as well as on the synchronization between excitatory inputs. Action potentials propagate along the axons towards the cell's presynaptic axonal terminals, where they transmit the all-or-none *output* of the neuron to its recipients. This transmission takes place via chemical neurotransmitters or neuromodulators that are released from vesicles into the synaptic cleft.

Most intracortical neurophysiological recordings are extracellular. This type of recording measures signals within the extracellular space that reflect both synaptic and spiking activity, without measuring neuronal membrane potentials directly. Most inactive neurons harbor a voltage gradient called the "resting potential" of about 60–70 mV across their lipid membranes by actively taking up certain anions via specialized ion pump membrane proteins. In other words, the inside of

a nonactive neuron is more negative than the extracellular medium. Current flow within a neuron is triggered when there is a membrane potential difference between two distinct regions of the neuron. This causes a return current flowing through the extracellular space in the opposite direction, in order to counter the internal neuronal current. Neuronal activity (for both input and output) is characterized by ionic current flow *between* the extracellular fluid and the intracellular compartment. Net negative (anionic) influx into a resting neuron hyperpolarizes that cell and makes its activation less likely, thus acting as an inhibitory current. Contrarily, neurons are more likely to reach the threshold of activation as positively charged (cationic) particles enter from the extracellular medium. This activation-dependent transmembrane current is akin to the removal of electric charge from the extracellular medium at the site of activation. Sites through which currents enter or leave a given system are termed a current source or a current sink, respectively. The sign of current is dependent on the perspective of the observer, and so is the definition of what constitutes a sink or source. When neurons are concerned, however, it has become customary to refer to excitatory (depolarizing) currents as a current sink. Thus, neuronal current sinks are typically localized at a site of synaptic excitation, where there is a net influx of positive ions. Net effluxes of positive ions in the form of passive return currents, forming the corresponding current source, occur at other regions of the same neuron, thus closing the local current loop (Nicholson 1973). The resulting electrical dipole forms the basis of the voltage difference that can be picked up by nearby microelectrodes. In other words, the temporal dynamics of the microscopic ionic fluxes produced by synaptic and spiking activity across the nerve cell membrane are summed to extracellular voltage fluctuations that can be recorded as the extracellular broadband signal.

The bulk of extracellular voltage established by activity in a large number of surrounding neurons can be measured with microelectrodes placed within the extracellular space in vivo and is referred to as local field potentials (LFPs). The highest fraction of the time-varying variance of extracellular voltage fluctuations occurs in the lowest frequency range (LFPs' magnitude falls off exponentially as a function of frequency). Given the predominance of low-frequency amplitude in their spectral composition, LFPs usually get analyzed in the frequency domain (i.e., in time-frequency analysis, or in frequency bands also used in classical EEG: delta, theta, alpha, beta, and gamma). However, the common use of the frequency domain to describe LFPs can also be somewhat misleading. Under some conditions, LFPs exhibit repeating patterns for limited periods of time, thus resembling actual oscillations. However, oscillatory LFPs are the exception rather than the norm. Most frequently, cortical LFPs exhibit no periodicity and therefore are better characterized as irregular fluctuations.

LFPs have proven to be a useful measure of brain activity as they provide an indication of (mostly) synaptic processes without the need for intracellular recordings. Nonetheless, LFPs are not perfect indicators of neuronal activity. LFPs arise from a multitude of neural events that cannot be easily disentangled and therefore create irresolvable ambiguity. Specifically, LFPs amplitudes depend on multiple factors, such as the strength of the synaptic input and its respective transmembrane

currents, as well as on the spatial distribution of the current sources and sinks, and the temporal synchrony of these events. The functional anatomy, position, and orientation of activated cells further influence the measured LFPs. For instance, a suitable stimulation of Purkinje cells in the cerebellum gives rise to large, coherent LFPs. This is also true of pyramidal cells in the cerebral cortex because their dendrites are predominantly parallel to each other. Certain classes of interneurons, on the other hand, do not contribute to LFPs to the same amount since their dendrites are distributed in a radial, star-shaped pattern that does not lend itself to linear spatial summation (Lauritzen 2005). Moreover, according to the relative timing of the neurons' action potentials and their geometrical arrangement, field potentials generated by two or more neurons may add up or cancel out. Nonetheless, synchronous activation of many parallel neurons within the brain will result in a large field potential (for reviews on field potentials, see Freeman 1975 and Logothetis 2002).

If the microelectrode is of suitable geometry and placed in the close vicinity of neurons, the slow-varying field potentials of the LFPs will be recorded simultaneously with scattered action potentials of nearby neurons. As discussed above, temporal filtering of the raw, broadband signal permits the dissociation of LFPs from spiking activity (Figures 6.1, 6.2). Signal content with frequencies above ~300 Hz and below ~150 Hz is taken to be the spiking activity of neurons (multiunit activity, MUA) and LFPs, respectively.

The frequency band separation between LFPs and spiking-related activity suggested above can be justified theoretically (Logothetis 2002). EPSPs and IPSPs are relatively slow events (10–100 ms long), in contrast to the fast waveform of neuronal action potentials (0.4–2 ms long). This temporal difference of neuronal events results in distinct power spectra for synaptic events compared to that of spikes. The average frequency spectrum of action potentials exhibits a power peak around 1 kHz, while that of simulated EPSPs shows substantially greater energy below 150 Hz. This difference prevails when comparing the frequency spectrum caused by a series of scattered synaptic events to the spectrum caused by spiking events.

Studies combining intra- and extracellular recordings lend further support to the notion that LFPs have a synaptic–dendritic origin (e.g., Pedemonte et al. 1998). Moreover, current source-density analysis (a technique that allows for the quantification of current flow within the neuropil) further indicates that LFPs correspond to a weighted average of synchronized dendro-somatic activity from a neural population within 0.5–3 mm of the electrode tip (Mitzdorf 1987; Juergens et al. 1999).

Given the combined theoretical and empirical support outlined above, it is reasonable to assume that LFPs mainly reflect synaptic events, including the synchronized synaptic input from afferent fibers as well as those originating from local neurons. While LFPs seem to represent a summation of synaptic activity from neurons within ~2 mm of the recording electrode tip, the MUA has been suggested to correspond to a weighted sum of the extracellular signatures of action potentials occurring within a ~200 μm radius from the electrode tip. The MUA is deemed to reflect primarily the action potentials of pyramidal cells, although action potentials from local interneurons, axons of passage, and dendrites may also play a role.

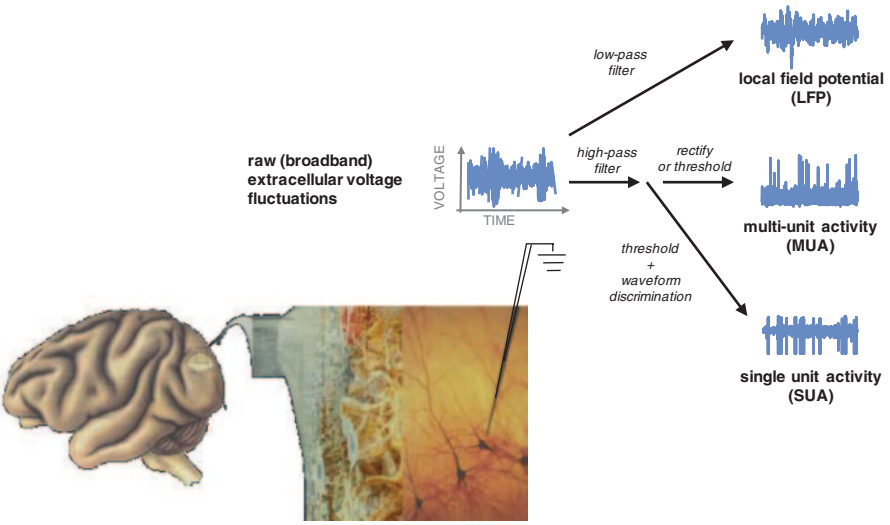

Fig. 6.1 Types of extracellular neurophysiological signals. Neurophysiologists commonly discriminate three major classes of signals that can be measured with microelectrodes placed inside the neuropil. (1) Depending on the material, geometry, and exact position of the probe, it is possible to isolate action potentials *(spikes)* of one or more isolated neurons. This single-unit activity *(SUA)* is quantified in a three-stage process. First, using band-limiting filters, the raw extracellular voltage gets narrowed down to a frequency band that matches the bandwidth of action potentials (~1 kHz). Next, occurrence of individual impulses gets marked by determining the time points at which the signal exceeded a certain threshold. In a final step, waveform analysis gets applied to discriminate individual neurons. (2) The activity of larger populations of neurons (multiunit activity, *MUA*) can be assessed by band-limiting the raw data to the frequency range of spiking activity, followed by either indiscriminate thresholding or by simple full-wave rectification in order to obtain the time-varying envelope of the band-limited signal. (3) Band-limiting the raw data into frequencies below the spectral range of spiking activity results in a signal called the local field potential, or *LFP*

Importantly, neocortical neurons are not spread out randomly. Instead, they are grouped together within a well-ordered laminar layout that largely repeats itself across the cortical mantle. This cortical lamination can be defined using a variety of histological staining techniques. The exact number of layers depends on the type of histological stain used and varies between cortical areas and individual species (DeFelipe et al. 2002). The resulting variability in layer count has prompted neuroanatomists to propose a variety of slightly differing labeling schemes (Billings-Gagliardi et al. 1974; Marín-Padilla 1998). However, the consensus follows neuroanatomist Korbinian Brodmann's (1868–1918) original plan of dividing the neocortex into six major laminae. These six basic layers often get grouped into three major laminar domains. In particular, layer 4 and its various sublayers are commonly referred to as the "granular layers" due to their fine-grained appearance in some histological stains. Accordingly, superficial layers 1–3 have been termed "supragranular," while deeper layers 5 and 6 get referred to as "infragranular" layers.

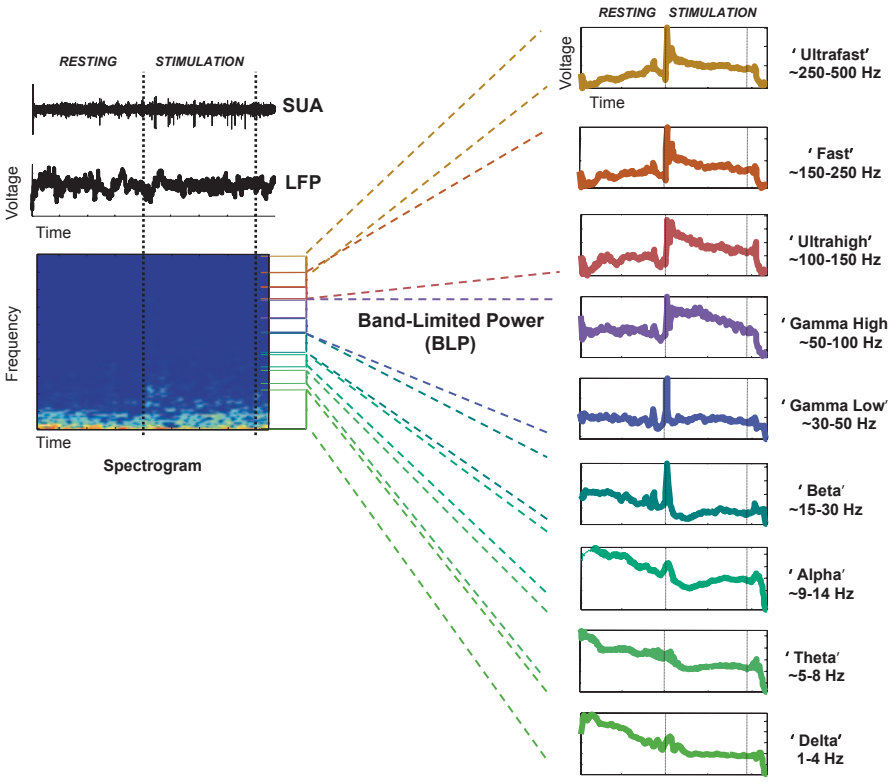

Fig. 6.2 Decomposition of LFP into frequency bands. The LFP represents a complex signal that is dominated by slow-varying, large-amplitude fluctuations. Averaging raw LFP, although informative, thus tends to overrepresent its low-frequency content. A common way to circumvent this bias is to break up the signal into its frequency components and study their evolution over time. This can be done either by (1) band-bass filtering the LFP into discrete frequency bands and estimating the band-limited power *(BLP)* or by (2) directly transforming the signal into the frequency domain using the Fourier Transform or related mathematical techniques. *SUA* single-unit activity

One motivation for the above labeling scheme is that the connection patterns between these three main laminar compartments as well as their interconnections with other cortical and subcortical sites are largely similar across the mammalian neocortex (but see, Haug 1987; Horton and Adams 2005; Nelson 2002). This observation has given rise to the hypothesis that there is a "canonical" blueprint to the cortical laminar circuitry that gets repeated stereotypically along the cortical sheet (Hubel and Wiesel 1974; Rockel et al. 1980). The basic schematic of signal flow across this stereotypical microcircuit of cortical layers has been mapped using a combination of anatomical and physiological techniques (e.g., Bode-Greuel et al. 1987; Nowak et al. 1995)). A consensus model derived from these studies (Douglas et al. 1989; Douglas and Martin 2004; Bannister 2005; Lübke and Feldmeyer 2007; Felleman and Van Essen 1991; Sotero et al. 2010) suggests that the bulk of the ascending information initially arrives at layer 4. Layer 4 neurons strongly project

to the supragranular layers, where the ascending information gets integrated with the cortico-cortical and subcortical inputs. The layer 2/3 efferences then project this integrated information to other cortical areas as well as to the infragranular layers. The layer 5/6 neurons back-project to the granular and supragranular layers, thus forming a reverberating loop between the superficial and deep cortical layers. The layer 5/6 neurons additionally convey this information to thalamic nuclei and other subcortical structures (Thomson and Bannister 2003).

The anatomical distinction of cortical layers outlined above is of direct relevance to the interpretation of fMRI signals. For one, neuroimaging has followed a steady trend towards laminar resolution as its spatial resolution continues to improve (e.g., Mittmann et al. 2011; Polimeni et al. 2010). However, the laminar differences of cortical organization are also relevant for fMRI data that lacks the spatial precision to differentiate between these laminae. In line with the anatomical separation of neurons throughout the cortical thickness, neurophysiological response differs along the same microscopic scales (Schroeder et al. 1998; Snodderly and Gur 1995; Bollimunta et al. 2008; Hansen and Dragoi 2011). Recent work has shown that the LFPs within the upper cortical layers (1–4) of monkey visual cortex, for example, share little commonality with LFPs in the lower two cortical layers. This functional separation holds for both ongoing activity and sensory stimulation (Maier et al. 2010, 2011; Buffalo et al. 2011). These results suggest that the heterogeneity of the cortical thickness needs to be taken into account when comparing neuronal signals to fMRI measurements.

Spatiotemporal Relationship Between Neuronal Activity and fMRI Signals

In the temporal domain, the BOLD response appears as a sluggish, low-pass filtered version of the neurophysiological response. The straightforward rationalization for this observation is that changes in blood flow occur on a slower timescale than changes in electrophysiological activity: BOLD responses transpire within hundreds of milliseconds to seconds, while the electrophysiological response may take place within milliseconds or tens of milliseconds following sensory stimuli. Considering the specific example of responses to a visual stimulus in the primary visual cortex (V1), for example, the onset of neuronal activity is within 20–50 ms, while a peak response takes place within 30–70 ms following the onset of the visual stimulus (Maunsell and Gibson 1992). The onset of the resulting vascular response lags 1.5–2.5 s behind the neuronal response. The measured onset of the corresponding BOLD response depends on the paradigm, the signal-to-noise ratio (SNR), the response magnitude, and the analysis parameters. Characteristically, peak blood flow and BOLD response are not achieved until 5–6 s after the exposure to the stimulus. Hence, a vascular response to a synaptic input can still be developing by the time a second stimulus arrives at the active region. To complicate matters even further, the vascular response to subsequent stimuli is influenced by preceding stimuli, due to the temporal overlap between responses (Lauritzen 2005).

In the spatial domain, the spatial specificity of fMRI signals is influenced by the choice of fMRI contrast and the strength of the magnetic field. It also depends on which aspect of the vasculature is being probed (e.g., capillaries, venules, or veins). The point-spread function of T2* BOLD response in the human visual area V1 has been estimated as ~3.5 mm at 1.5 T (Engel et al. 1997) and less than 2 mm at 7 T (Shmuel et al. 2007; see Chap. 26) The point-spread function of T2 and T2* BOLD responses at 7 T relative to metabolic activity have been estimated as~0.8 mm and ~1.0 mm, respectively (Chaimow et al. 2015).

Correlations Between Neurophysiological Activity and fMRI Responses

The vast majority of studies analyzing the link between neuronal, metabolic, and hemodynamic responses have reported a monotonic (or even linear) increase in metabolic and hemodynamic activity following increases in neural activity. For example, relative changes in the level of blood oxygenation in cat area 18 are proportional to increases in neuronal activity during the first phase (the "initial dip") of the associated metabolic and hemodynamic response (Shmuel and Grinvald 1996; Fig. 6.3a). Likewise, a study in rat somatosensory cortex illustrated that the rate of oxygen consumption is proportional to increases in neuronal activity during the late phase of the hemodynamic response (Smith et al. 2002; Fig. 6.3b). It has also been shown that the CBF response to stimulation of climbing fibers in the rat cerebellum is proportional to the integrated neuronal responses induced by that stimulation (Mathiesen et al. 1998).

The amplitudes of somatosensory-evoked potentials were found to linearly correlate with the BOLD responses in rat sensory cortex when activated by forepaw stimulation across a range of stimulus frequencies (Brinker et al. 1999). An analogous conclusion was reached in humans after observing the hemodynamic response to stimulation of the median nerve using different stimulus intensities (Arthurs and Boniface 2003). In the monkey, visual stimuli with different luminance contrasts elicited BOLD responses that were proportional to the corresponding increases in neuronal activity (Logothetis et al. 2001).

In addition to the linear relationship between the electrophysiological and vascular responses observed in the studies outlined above, other studies found evidence for nonlinear relationships between these two measures. The CBF response to the stimulation of parallel fibers within the cerebellum has shown a sigmoidal relation to the summated increases in neuronal activity (Mathiesen et al. 1998; Fig. 6.4). Devor et al. (2003) combined optical measurements of hemodynamic signals with simultaneous recordings of neural activity and demonstrated a nonlinear relationship between neuronal and hemodynamic responses in an event-related paradigm. Specifically, the hemodynamic response continued to increase with stimulus intensity beyond the point of saturation of the electrical activity. Jones et al. (2004) and Sheth et al. (2004) reported similar observations. In the latter study, both a nonlinear power law or threshold models better described the neurovascular coupling in

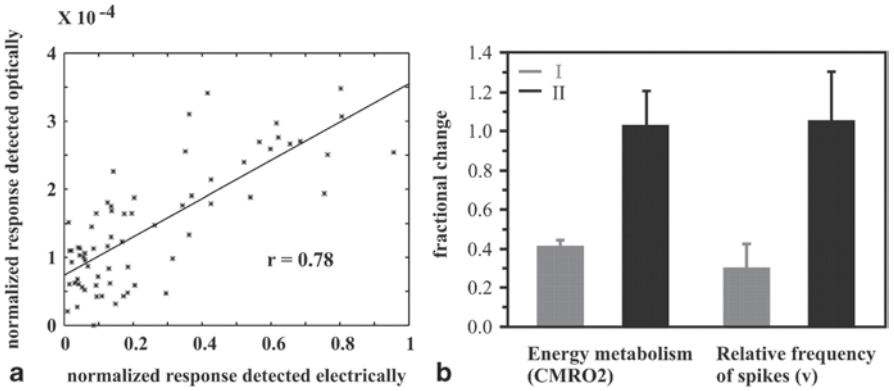

Fig. 6.3 Association between oxygen consumption and spiking activity. **a** Correlation between changes in blood oxygenation measured optically and the underlying action potential activity. These data were taken during the initial phase ("initial dip") of the response. Linear regression was used to generate the best linear fit to the data, which shows a high degree of linearity. Modified from Fig. 7 of Shmuel and Grinvald (1996) with permission. **b** Stimulation of the rat forepaw led to comparative changes in oxygen consumption and spiking activity. Responses obtained from baseline conditions I and II are shown in *gray* and *black,* respectively. The baseline condition II was lowered by ~30% from baseline condition I due to a higher dosage of α-chloralose; however, the incremental response from condition II was larger. In both modalities, oxygen metabolism and spiking activity, the same levels of activation were approximately reached upon stimulation from the two different starting baseline levels. *CMRO2* cerebral metabolic rate of oxygen. Modified from Fig. 3 of Smith et al. (2002) with permission

rat somatosensory cortex than linear models. Hoffmeyer et al. (2007) examined neurovascular coupling in rat sensory cortices in response to direct stimulation of transcallosal pathways. They showed that an exponential relation exists between CBF responses and the summed amplitudes of neuronal activity. Nielsen and Lauritzen (2001) observed yet another type of nonlinearity, suggesting that a certain minimum threshold of coordinated synaptic activity must be reached in order to trigger a hemodynamic response. The relationship found in that study suggests that small changes in neuronal activity may be undetectable by perfusion-based imaging techniques. Hence, synaptic activity needs to surpass a minimum threshold in order to cause an increase in CBF.

Overall, it appears that within a limited dynamic range of stimulus conditions, hemodynamic signals couple linearly to neuronal activity. In some neural networks, however, the hemodynamic responses become saturated before the neuronal activity reaches its maximum, such that a further increase in neuronal activity does not induce further increases in the hemodynamic response. Therefore, simply subtracting fMRI signal strengths obtained during two experimental conditions might not properly indicate the relative difference in overall neuronal activity between the two states (Lauritzen 2005).

Interpreting fMRI data is complicated not only by the partially nonlinear relation between hemodynamics and neural activity but also by differences in the SNR. The SNR of the neurophysiological signal associated with induced neuronal activity is about two orders of magnitude greater than that of the BOLD signal (Logothetis

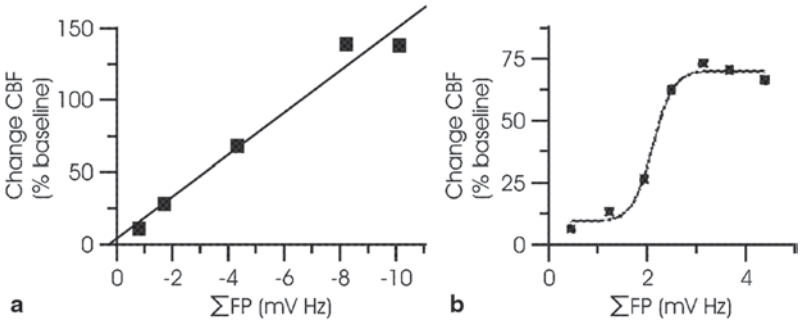

Fig. 6.4 Relationship between neuronal and hemodynamic responses in rat cerebellum. **a** Frequency-dependent CBF increases in response to climbing fibers stimulation are correlated with the sum of active and passive postsynaptic activity. The figure presents the scatter plot of increases in CBF versus summed field potentials (i.e., the product of field potential amplitudes and stimulation frequency). The line demonstrates the results of linear regression ($r=-0.985$, $P=0.0022$). **b** Stimulation of parallel fibers at increasing frequencies leads to increases in summed field potentials and increases in CBF responses. The figure presents increases in CBF (*ordinate*) versus summed field potentials (*abscissa*) from one rat, illustrating a sigmoidal relationship between the two variables. CBF cerebral blood flow. Both panels were modified from Mathiesen et al. (1998) (Figs. 4d and 5d) with permission

et al. 2001). Such a difference can, among other things, lead to the statistical rejection ("false negative") of valid activity during mapping experiments, despite the fact that the underlying neural response is significant. These conclusions are consistent with the demonstration that extensive averaging of fMRI data allows more brain regions to be correctly classified as activated regions (Saad et al. 2003).

What is the Neural Origin of Hemodynamic Responses?

As indicated above, several studies have found a roughly linear relationship between the metabolic and hemodynamic responses and local spiking activity. Shmuel and Grinvald (1996) compared the optically measured reduction in blood oxygenation (the "initial dip") in gray matter regions to the action potential response to visual stimuli of drifting gratings using optical imaging of intrinsic signals in juxtaposition with extracellular recordings in cat area 18. They observed an approximately linear relationship between these two measures that suggests a correspondence between the oxygen consumption during the initial phase of the BOLD response, before the increase in CBF, and spiking activity. Smith et al. (2002) recorded changes in the spiking activity of neuronal ensembles during forepaw stimulation of anesthetized rats and found a similar connection between oxygen consumption and spiking activity for the subsequent phase of the positive BOLD response following the increase in CBF. They furthermore derived the localized changes in oxygen consumption, under the same conditions, from BOLD fMRI data in combination with measured changes in CBF and cerebral blood volume (CBV). The variations in oxygen con-

sumption were reported to be roughly proportional to the associated changes in spiking activity.

Rees et al. (2000) compared fMRI responses induced by visual motion stimuli in human area MT+ to spike rates obtained from single neurons in monkey MT using matching stimuli. Responses in human MT+ showed a strong and highly linear dependence on the coherence of motion signals, which was akin to the responses of action potentials obtained from the monkeys with the same stimuli. Similar results were obtained by comparing BOLD responses in human V1 and action potential responses in monkey V1 to stimuli of varying luminance contrast (Heeger et al. 2000). These observations support the notion that fMRI responses of a cortical area are directly proportional to the average firing rate of its local cell population.

However, synaptic activity is highly interrelated with the firing rates of presynaptic and postsynaptic neurons under physiological conditions. This suggests that synaptic activity is also correlated with the local metabolic and hemodynamic responses. This is particularly valid in case of the cerebral cortex, where the majority of synapses (both excitatory and inhibitory) can be traced to a local network of connections originating in a nearby cortical neighborhood, thereby leaving only a minority of inputs from more remote cortical and subcortical structures (Braitenberg and Schuz 1991; Peters and Payne 1993; Peters and Sethares 1991). We can therefore expect that an increase in the average firing rate correlates with a comparative rise in local synaptic activity, which in turn leads to an increase in both the metabolic demand and vascular response.

Given the above, it may not be surprising that in many cases, the BOLD signal has been found to correlate equally well with LFPs and spiking activity. For example, Mukamel et al. (2005) contrasted single-unit activity and LFPs in the auditory cortex of two neurosurgical patients with the fMRI signals of healthy subjects during the presentation of an identical movie segment. The findings revealed a linear relationship between spiking activity, high-frequency LFPs, and the fMRI BOLD signal measured in human auditory cortex during natural stimulation. However, since the spiking activity also was highly correlated with the high-frequency LFP, the results cannot answer the question as to which signal has more predictive power for estimating the local BOLD response.

To summarize the above, the BOLD fMRI signals can be taken as a dependable estimate of the average firing rate of the underlying neuronal population under a wide variety of stimulation conditions. However, correlation does not equal causation. The mere observation of close coupling between these signals does not imply that spiking activity drives the BOLD signal. One problem in particular is that the level of local synaptic activity (and the resulting LFPs) tends to be closely associated with simultaneous changes in spike rate. It is difficult to attribute the relative roles of synaptic inputs versus the spiking output for hemodynamic changes given that both these processes tend to covary that closely. However, several studies managed to separate the different types of neurophysiological measures outlined above in order to investigate their relative effects on the BOLD response.

Schwartz et al. (1979) measured regional brain glucose metabolism in rats using 2-deoxyglucose autoradiography (Sokoloff et al. 1977). They subjected rats to an osmotic load that was sufficient to stimulate cell bodies in the supraoptic

and paraventricular nuclei of the hypothalamus. Importantly, the axon terminals of these nuclei reside in the posterior pituitary gland—a considerable distance from the stimulated cell bodies. The authors compared the metabolic activity in the two locations and found that metabolism increased significantly in the area harboring the axon terminals in the posterior pituitary gland but did not measurably change in the cell bodies residing in the hypothalamus. This finding is consistent with the known relationship between the metabolic cost of sustaining ionic gradients and the surface-to-volume ratio of the involved cellular elements (Cohen and De Weer 1977; Ritchie 1967; Raichle and Mintum 2006). In general, their data support the notion that the synaptic input, and not the spiking activity, is the driving mechanism of CBF (see Lauritzen 2005, for additional evidence).

Mathiesen et al. (1998) employed laser Doppler flow and extracellular neurophysiological measurements to differentiate between synaptic and spiking activity in order to investigate their relative impact on CBF in the rat cerebellum. Stimulation of the monosynaptic climbing fiber system triggered extracellular field potentials and complex spikes in Purkinje cells with concurrent increases in CBF. However, when spiking activity of the Purkinje cells was inhibited as a result of stimulation of the disynaptic parallel fiber system, CBF increased despite the decrease in spiking activity (Fig. 6.5a). This discovery verified that activity-dependent CBF increases in the cerebellum depend on synaptic excitation, which includes excitation of inhibitory interneurons. In contrast, the net spiking activity of Purkinje cells is insignificant for the vascular response.

More recently, Thomsen et al. (2004) examined the consequences of enhanced spike activity on CBF in rat cerebellum under conditions of disinhibition, which was achieved by blocking GABA(A) receptors with either bicuculline or picrotoxin. Disinhibition increased Purkinje cell-spiking rates to 200–300 % of control activity, without incurring an increase in basal CBF. This illustrates that increased spike activity alone is insufficient in affecting CBF. However, neurovascular coupling between excitatory synaptic activity and CBF responses evoked by climbing fiber stimulation was maintained during disinhibition. Hence, the unaffected CBF in the presence of increased Purkinje cell-spiking rate could not be accounted for by impaired synaptic activity–CBF coupling. Thus, increasing spiking of principal neurons is neither sufficient nor essential to elicit CBF responses. Instead, activation-dependent vascular signals seem to mainly reflect excitatory synaptic activity (Fig. 6.5).

Logothetis et al. (2001) examined the relationship of the BOLD signal to LFPs and spiking activity in monkey visual cortex. The largest increases in power in response to visual stimulation were observed within the gamma frequency range (>30 Hz) of the LFPs. LFPs were found to reflect the time course of the BOLD response more accurately since it tended to remain elevated for the duration of the visual stimulus, whereas the spiking activity did not (Fig. 6.5b). Correspondingly, linear systems analysis revealed that LFPs yield a better approximation of the BOLD response than the spiking responses. A similar study in alert monkeys verified that LFPs are more accurate and more reliable predictors of the BOLD response, despite the fact that both LFPs and MUA correlate with the BOLD signal (Goense and Logothetis 2008).

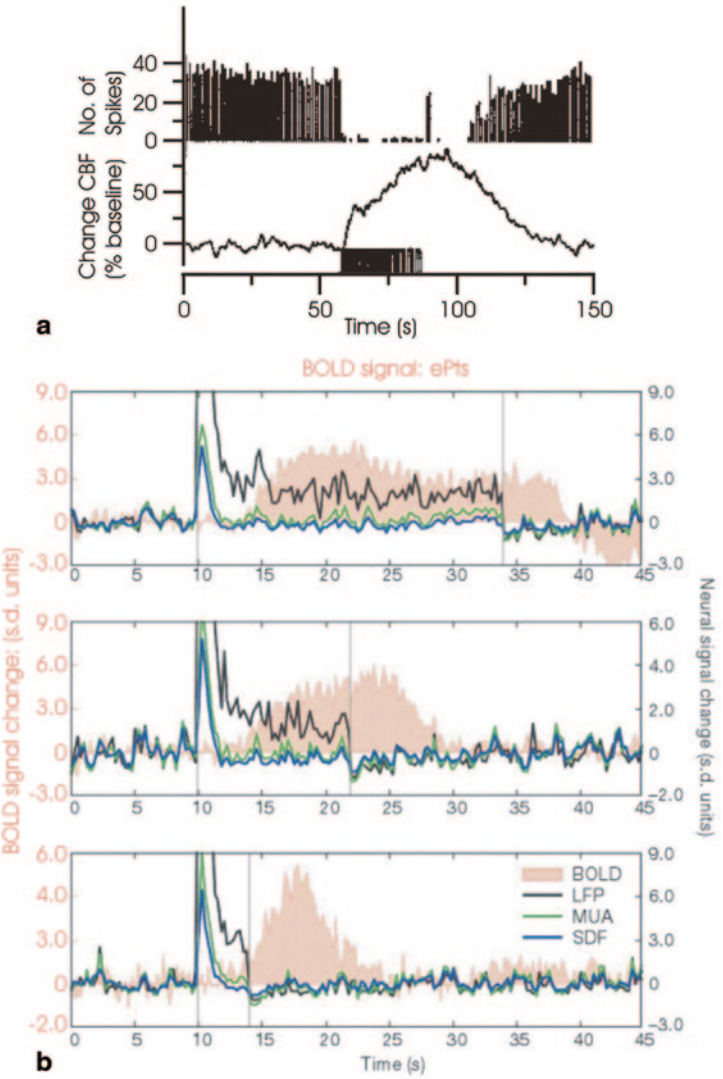

Fig. 6.5 CBF and BOLD responses correlate with LFPs. **a** Activity-dependent CBF increases and spike activity in response to parallel fiber stimulation in the cerebellum. Purkinje cell-spiking activity diminished after 1–3 s of stimulation, and spontaneous firing did not return to baseline until 19–25 s after the end of stimulation *(upper plot)*. CBF increased during stimulation and persisted for 5–10 s after the end of stimulation before returning to baseline after a lag of 40–50 s *(lower plot)*. Modified from Fig. 3a of Mathiesen et al. (1998) with permission. **b** Simultaneous neural and BOLD recordings from a cortical site showing a transient MUA response. Responses to a pulse stimulus of 4, 12, 24 s are shown in the bottom, middle, and *top* plots, respectively. LFP is the sole signal showing time course matched in response duration with that of the BOLD response. Both the spike density function *(SDF)* and the multiunit responses *(MUA)* adapt back to baseline a couple of seconds after stimulus onset. The BOLD time series is from an ROI around the electrode. *CBF* cerebral blood flow, *ROI* region of interest. Modified from Fig. 3 of Logothetis et al. (2001) with permission

Similar results were reported by Niessing et al. (2005), who measured neurophysiological and optically recorded hemodynamic responses in the cat visual cortex. Increasing the stimulus strength resulted in enhanced spiking activity, high-frequency LFPs power, and hemodynamic responses. However, hemodynamic responses were shown to fluctuate when stimuli of constant intensity were presented to the animal. These fluctuations were only weakly related to the rate of action potentials and tightly associated with LFPs power in the gamma range. When sorting all trials according to the amplitude of the hemodynamic response, clear differences were detected with respect to the frequency distribution of the respective LFPs. Power increases in the delta- (~1–4 Hz), theta- (~4–7 Hz), and the alpha (~8–12 Hz) frequency band were most prevalent in trials with the weakest optical responses. With increasing hemodynamic response, the peak of LFPs power shifted from the theta and alpha band to the beta (~12–30 Hz) and lower gamma frequency band. The strongest hemodynamic responses were linked with high power in the lower and upper gamma frequency band. Quantifying the relationship between the strength of the hemodynamic response and the LFPs power in different frequency bands revealed that low-frequency activity in the delta band was negatively correlated with hemodynamic signal strength. Theta, alpha, and beta power was not significantly correlated with this signal. A weak and strong positive correspondence existed for LFPs power in the lower and upper gamma band, respectively. LFPs power in the high-frequency range in particular is thought to increase with the local synaptic events, signifying a close association between hemodynamic responses and neuronal synchronization.

Viswanathan and Freeman (2007) demonstrated yet another dissociation between synaptic and spiking activity in the cat primary visual cortex. They presented visual stimuli composed of gratings that were drifting at different temporal frequencies while simultaneously recording neural responses and tissue oxygenation, which can serve as a proxy to the BOLD signal. Spiking activity decreased while LFPs power in the lower gamma band became more prevalent when the temporal frequency of the gratings was increased. Compared to their maximal responses obtained at 4 Hz, spiking activity and low-gamma LFPs responses dropped to approximately 15% and 85%, respectively, during visual stimulation at 20 Hz. LFPs responses in the delta, theta, alpha, beta, and high-gamma bands plunged to approximately 40% of their maximal response at 4 Hz, while the tissue oxygen fell to 60%. These results indicate the existence of close coupling between tissue oxygenation and LFPs power in the low-gamma band.

More recently, Rauch et al. (2008) induced an experimental dissociation between MUA and LFPs activity with injections of a neuromodulator that primarily acts on efferent neuronal membranes into the primary visual cortex of anesthetized monkeys. Its infusion in the visual cortex consistently reduced MUA responses without significantly affecting either LFPs or BOLD activity, implying that the efferent neurons within visual cortex pose a relatively small metabolic burden compared to the overall presynaptic and postsynaptic processing of incoming afferents. In other words, BOLD seems to predominantly reflect presynaptic and postsynaptic processing of incoming afferents to a particular region.

So far, we have described both cases of coupling and of dissociation between spiking activity and the BOLD signal. However, the question remains: What determines whether the BOLD signal is associated with or dissociated from the spiking output of neurons in any specific paradigm? With the help of multiple electrodes in the human auditory cortex, Nir et al. (2007) measured isolated unit activity and LFPs, and observed a wide range of coupling levels between the activity of individual neurons and gamma-range LFPs. Gamma LFPs were well correlated to BOLD signals measured across different individuals ($r = 0.62$). The coupling of single units to BOLD was highly variable in comparison, but tightly related to interneuronal firing-rate correlations ($r = 0.70$). These results suggest that the BOLD signal could reflect the output spiking activity depending on whether the paradigm evokes a high degree of interneuronal correlation.

Neuronal Correlates of NBRs

Sustained negative responses are pervasive in functional imaging. Some hypotheses regarding the origin of these negative responses suggest a purely vascular basis for this phenomenon (such as "vascular blood steal"), concluding that the NBR bears little relation to the underlying neuronal activity (Harel et al. 2002; Kannurpatti and Biswal 2004). Shmuel et al. (2002) demonstrated a robust, sustained NBR in the human occipital cortex triggered by stimulating part of the visual field. The NBR was linked with decreases in CBF and oxygen consumption. These results suggest that the NBR is associated with reduction in neuronal activity. More recently, similar connections of NBRs with decreases in CBF and oxygen consumption have been reported in the visual (Uludağ et al. 2004; Pasley et al. 2007) and motor cortices (Stefanovic et al. 2004, 2005). In addition, Shmuel et al. (2006) employed an analogous stimulation paradigm to the one they used in humans in order to obtain an NBR beyond the stimulated regions of the monkey primary visual cortex. Using simultaneous fMRI and electrophysiological recordings, these authors showed that the NBR was associated with local decreases in neuronal activity below the baseline level of spontaneous activity. Trial-by-trial amplitude fluctuations showed tight coupling between the NBR and reduced neuronal activity. The NBR was linked to comparable decreases in LFPs and MUA. These findings indicate that a large component of the NBR stems from decreases in neuronal activity (Fig. 6.6).

More recently, the neuronal and vascular mechanisms underlying NBRs were studied by Devor et al. (2007) using optical imaging techniques in rat primary somatosensory cortex. Stimulation of the rat forepaw evoked a central region of net neuronal depolarization surrounded by net hyperpolarization. Hemodynamic measurements revealed the correspondence between depolarized regions with an increase in oxygenation as well as an association between hyperpolarized regions with a decrease in oxygenation. On the microscopic level of single-surface arterioles, the response was composed of a combination of dilatory and constrictive phases. The relative strength of vasoconstriction covaried with the relative strength of neuronal hyperpolarization and the corresponding decrease in oxygenation. These

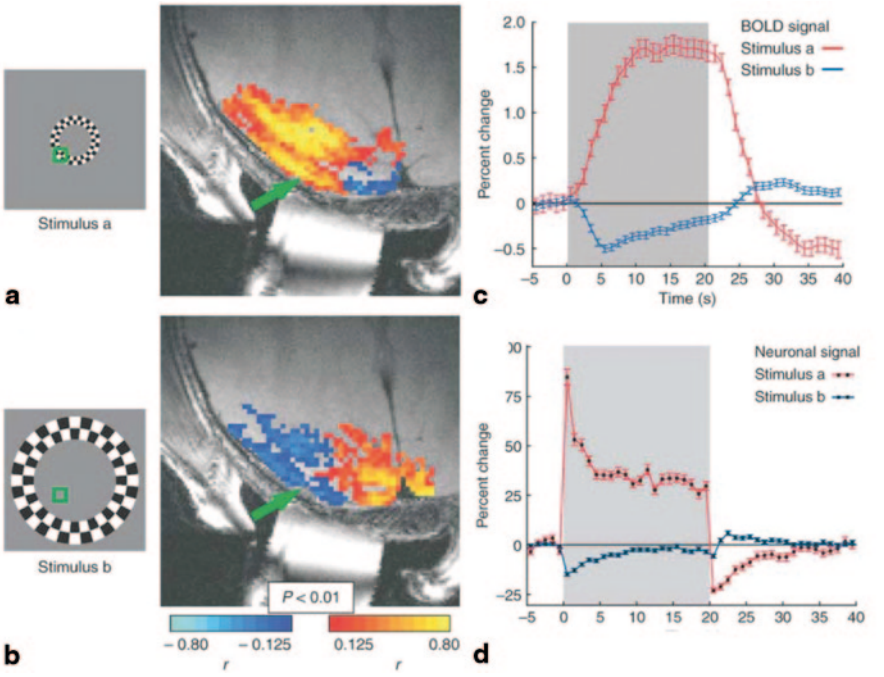

Fig. 6.6 Neuronal correlates of a negative BOLD response *(NBR)*. **a**, **b** Patterns of response to a central and a peripheral visual field stimulus, respectively. The fMRI response from a single axial-oblique slice is superimposed on the corresponding anatomical image. *Green arrows* indicate position of the recording electrode within visual area V1. *Green squares* represent the collective receptive field of the neurons in the vicinity of the electrode. The stimulus in **a** overlapped with the receptive field, invoking a positive BOLD response in the area directly surrounding the electrode. The stimulus in **b** did not overlap with the receptive field and induced an NBR in that same vicinity. **c** Time course (mean±SEM) of the BOLD response sampled from the ROI around the electrode. **d** Neuronal responses to the stimuli presented in **a** and **b**. Time courses (mean±SEM) present the fractional change in power of the broadband neuronal signal in response to stimuli that overlapped *(red)* or did not overlap *(blue)* with the receptive field. The data in **c** and **d** were averaged over all trials from 15 sessions. All panels were modified from Shmuel et al. (2006) (Figs. 1a, b, d and 2a) with permission

conclusions imply that neuronal inhibition and concomitant arteriolar vasoconstriction relate to a decrease in blood oxygenation, which would be consistent with a negative BOLD fMRI response.

Additional evidence linking NBRs with suppression of neurophysiological activity was demonstrated by Boorman et al. (2010). These authors employed electrical whisker-pad stimulation while imaging the rat somatosensory cortex. They demonstrated NBR in deeper cortical layers relative to the positive BOLD response. Separate two-dimensional optical imaging spectroscopy and laser Doppler flowmetry revealed that the NBR was a result of decreased blood volume and flow and increased levels of deoxyhemoglobin. Neural activity in the NBR region, measured by multichannel electrodes, varied considerably as a function of cortical depth.

There was a decrease in neuronal activity in the deep cortical laminae. After cessation of whisker stimulation there was a large increase in neural activity above baseline. Both the decrease in neuronal activity and increase above baseline after stimulation cessation correlated well with the simultaneous measurement of blood flow suggesting that the NBR is related to decreases in neural activity within the deep cortical layers.

Neuronal Correlates of Spontaneous Fluctuations in fMRI Signals

Early human fMRI studies deemed that the large cortical signal fluctuations that can be seen when a subject is resting without explicit stimulation or a task inside the MR scanner are meaningless "noise." However, recent work has demonstrated that the spatio-temporal structure of these spontaneously occurring signal changes is not random: It is highly organized and consistent between subjects (Biswal et al. 1995; Fox and Raichle 2007). Therefore, the relationship between the BOLD response and the underlying neural events in the resting state is of a particular interest. These spontaneous fluctuations in fMRI signals are reminiscent of previously demonstrated spontaneous fluctuations in cortical neuronal signals obtained from cats (Arieli et al. 1996) and monkeys (Leopold et al. 2003). Importantly, these resting-state fluctuations are correlated over large parts of the human brain (Biswal et al. 1995), a phenomenon termed functional connectivity. Several studies identified contributions of nonneuronal origin to spontaneous fluctuations in fMRI signals. These contributions include vascular vaso-motion (Mayhew et al. 1996) and respiration (Birn et al. 2006; Wise et al. 2004).

Shmuel and Leopold (2008) utilized simultaneous fMRI and intracortical neurophysiological recordings in anesthetized, paralyzed monkeys, either staring at a uniform gray field or in complete darkness. They demonstrated, under both conditions, an association between the slow fluctuations in BOLD signals and concurrent fluctuations in the underlying local neuronal activity. This correlation varied with the BOLD signal time lag relative to neuronal activity, resembling a traditional hemodynamic response function with peaks at a 6-s lag of the BOLD signal (Fig. 6.7a–j). These associations were consistently identified when the neuronal signal consisted of either relative power variations in the LFPs gamma band, MUA, or the spiking rate of a small group of neurons. Further examination of the relationship between the voxel-by-voxel fMRI time series and the neuronal activity measured within one cortical site revealed that widespread areas of the visual cortex in both hemispheres were significantly correlated with neuronal activity from a single recording site in V1 (Fig. 6.7k). Assuming that Shmuel and Leopold's (2008) conclusions based on results in V1 can be generalized to other cortical areas, fMRI-based functional connectivity between remote regions in the resting state can be linked to synchronization of slow fluctuations in the underlying neuronal signals.

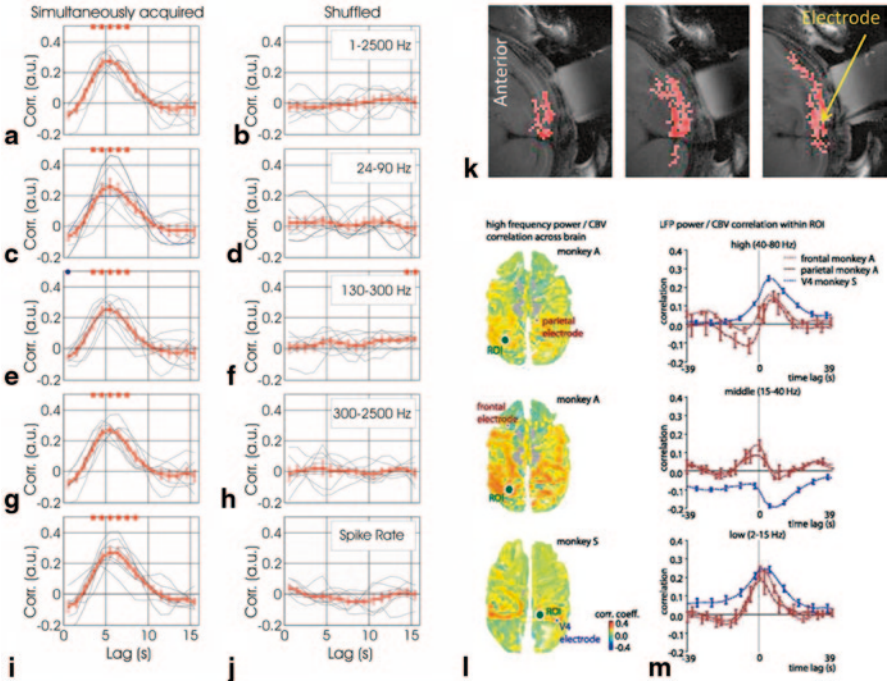

Fig. 6.7 Spontaneous fluctuations in BOLD signal correlate with the underlying neurophysiological activity. **a–i** Covariation between spontaneous fluctuations in fMRI and neuronal signals as a function of temporal lag. **a** The *gray curves* show the correlation as a function of lag from each experiment. The *red curve* presents the correlation function averaged over seven experiments in five different monkeys (mean ± SEM). The vertical axis represents the Spearman's correlation coefficient between BOLD and the fluctuations in relative (fractional change) power averaged over frequencies of the denoised broadband neurophysiological signal acquired simultaneously with fMRI. The horizontal axis represents the lag between the two correlated signals, with positive lags standing for BOLD lagging behind the neuronal activity. **b** Correlation between the same signals as presented in (**a**), computed after breaking the simultaneity condition by shuffling the segments of BOLD and neuronal activity obtained within each experiment. **c–h** Present correlation functions in the format used for (**a**) and (**b**), for the LFP, mid-range, and MUA bands, respectively. **i** and **j** Present similar correlation functions for fluctuations in spiking activity, estimated by counting identified action potentials over 1-s epochs rather than using frequency-based analysis. Modified from Shmuel and Leopold (2008), with permission. **k** Spatial extent of the correlation between the slow relative fluctuations in power averaged over the frequencies of the broadband neuronal signal recorded at the tip of the electrode *(yellow arrow)* and the fluctuations in BOLD measured voxel by voxel. Pink-colored voxels showed statistically significant positive correlation between the neurophysiological activity recorded in one site in V1 and BOLD signals for a 5-s time lag (t test, averaging over the correlation obtained time segment by time segment, $p < 0.01$). Modified from Shmuel and Leopold (2008), with permission. **l** Spatial extent of the fMRI correlation with high-frequency LFP in frontal area 6d, parietal area 7a, and occipital area V4. **l** In all cases, spatial correlations are bilateral and spread over large swathes of the cerebral cortex. **m** Cross-correlation functions between the fMRI (region of interest, ROI, data) and LFP power time courses for three electrodes outside V1 and for the three LFP frequency ranges: low (2–15 Hz), middle (15–40 Hz), and high (40–80 Hz). Modified from Schölvinck et al. (2010), with permission. *CBV* cerebral blood volume, *LFP* local field potential

More recently, Schölvinck et al. (2010) reproduced and expanded on these results in alert monkeys. Their results demonstrate the widespread, positive correlations of fMRI signals, over nearly the entire cerebral cortex, with the spontaneous fluctuations in the LFPs measured from a single cortical site (Fig. 6.7). The spontaneous neural activity reported in that study accounted for 10% of the observed BOLD signal variance, which is a considerable fraction of the 50% explained variance during visual stimulation. Similarly to the findings by Shmuel and Leopold (2008), the observed correlation was especially consistent in a band of upper gamma-range frequencies (40–80 Hz; Fig. 6.7m). A strong, positive correlation was also detected in a band of lower frequencies (2–15 Hz), albeit with a lag closer to zero. Overall, these findings specify that the global constituent of fMRI fluctuations measured during the resting state is closely linked with underlying neural activity.

Dissociations Between BOLD Responses and Neurophysiological Activity

The previous sections focused on cases that reported metabolic and hemodynamic responses that corresponded to changes in neurophysiological activity. A few studies reported cases in which these signals dissociated. Maier et al. (2008) investigated a paradigm in which a visual stimulus may become subjectively invisible. Perceptual disappearance of the visual stimulus elicited a robust drop in area V1 fMRI signal in humans. In contrast, monkey single-unit recordings failed to demonstrate such perception-locked changes in V1. To investigate the basis of this discrepancy, they measured both the BOLD response and electrophysiological signals in two monkeys. They found that all signals were in good agreement during conventional stimulus presentation, showing strong modulation to the presentation and removal of a stimulus. During perceptual suppression, however, only the BOLD response and the low-frequency (5–30 Hz) LFPs power showed decreases, whereas the spiking and high-frequency LFPs power remained unaffected. These results demonstrate that the coupling between the BOLD and electrophysiological signals in V1 is context dependent, with a marked dissociation occurring during perceptual suppression.

While Maier et al. (2008) did observe changes in lower frequencies bands that did correspond to the changes in BOLD signal, Sirotin and Das (2009) found evidence of a complete divergence of hemodynamic and neurophysiological signals. Using a dual wavelength optical imaging technique that independently measures CBV and oxygenation, they found two distinct components to the hemodynamic signal in the alert animals' primary visual cortex (V1). One component was reliably predictable from neuronal responses generated by visual input. The other component, of almost comparable strength, was reported as an unknown signal that entrains to task structure independently of visual input or of standard neural predictors of hemodynamics. The resulting data exhibited robust modulations of the hemodynamic signal at the trial frequency, even though the animals were virtually in total darkness and

foveal V1, the only region receiving visual input from the fixation point, lay outside of the imaged area. This latter component showed predictive timing, with increases of CBV in anticipation of trial onsets even in darkness. Sirotin and Das (2009) suggested the existence of a preparatory mechanism that brings additional arterial blood to cortex in anticipation of expected tasks, managed by distal neuromodulatory control of cerebral arteries. However, this interpretation was challenged in a few commentaries (e.g., Logothetis (2010) and Handwerker and Bandettini (2011)), indicating that in fact the data presented by Sirotin and Das (2009) showed modulation of neuronal activity in V1, likely reducing spontaneous activity during fixation. The increased inhibition, visible in their spectrograms, may trigger CBV changes and yield the anticipatory responses. It was hypothesized that the responses are due to site-specific effects of neuromodulatory input on the cortical excitation–inhibition balance, mediated by norepinephrine released from the locus coeruleus. Others (e.g., Tan 2009) supported the findings and interpretation of Sirotin and Das (2009) and suggested that the task-related properties of these responses point to a possible link between regional cerebral microcirculation and dopaminergic signaling. It was hypothesized that dopamine plays a role in task-dependent, "on-demand" allocation of metabolic resources.

Note that both Maier et al. (2008) and Sirotin and Das (2009) pursued their measurements in alert animals, in contrast to the majority of other studies of neurovascular coupling that used anesthetized animals. This indicates that neurovascular coupling may be modified in the alert state, possibly via the action of neuromodulators that depend on the behavioral state. This finding adds to the complexity of the interplay between neurophysiological signals and hemodynamic responses, which surely will be addressed in future studies.

Acknowledgments Authors would like to thank Dr. Vivien Casagrande for helpful comments on an earlier version of the section on cortical neuroanatomy.

References

Arieli A, Sterkin A, Grinvald A, Aertsen A (1996) Dynamics of ongoing activity: explanation of the large variability in evoked cortical responses. Science 273:1868–1871

Arthurs OJ, Boniface SJ (2003) What aspect of the fMRI BOLD signal best reflects the underlying electrophysiology in human somatosensory cortex? Clin Neurophysio. 114:1203–1209

Bandettini PA, Wong EC, Hinks RS, Tikofsky RS, Hyde JS (1992) Time course EPI of human brain function during task activation. Magn Reson Med 25:390–397

Bannister AP (2005) Inter- and intra-laminar connections of pyramidal cells in the neocortex. Neurosci Res 53:95–103

Billings-Gagliardi S, Chan-Palay V, and Palay SL (1974) A review of lamination in area 17 of the visual cortex Macaca mulatta. J Neurocytol 3:619–629

Birn RM, Diamond JB, Smith MA, Bandettini PA (2006) Separating respiratory-variation-related fluctuations from neuronal-activity-related fluctuations in fMRI. Neuroimage 31:1536–1548

Biswal B, Yetkin FZ, Haughton VM, Hyde JS (1995) Functional connectivity in the motor cortex of resting human brain using echo-planar MRI. Magn Reson Med 34:537–541

Bode-Greuel, KM, Singer W, Aldenhoff JB (1987) A current source density analysis of field potentials evoked in slices of visual cortex. Exp Brain Res 69:213–219

Bollimunta A, Chen Y, Schroeder CE, Ding M (2008) Neuronal mechanisms of cortical alpha oscillations in awake-behaving macaques. J Neurosci 28:9976–9988

Boorman L, Kennerley AJ, Johnston D, Jones M, Zheng Y, Redgrave P, Berwick J (2010) Negative blood oxygen level dependence in the rat: a model for investigating the role of suppression in neurovascular coupling. J Neurosci 30:4285–4294

Braitenberg V, Schuz A (1991) Anatomy of the cortex. Springer, Berlin

Brinker G, Bock C, Busch E, Krep H, Hossmann KA, Hoehn-Berlage M (1999) Simultaneous recording of evoked potentials and T2*-weighted MR images during somatosensory stimulation of rat. Magn Reson Med 41:469–473

Buffalo EA, Fries P, Landman R, Buschman T J, Desimone R (2011) Laminar differences in gamma and alpha coherence in the ventral stream. Proc Natl Acad Sci U S A 108:11262–11267

Buxton RB, Uludağ K, Dubowitz DJ, Liu TT (2004) Modeling the hemodynamic response to brain activation. Neuroimage 23:S220–S233

Cauli B, Tong XK, Rancillac A, Serluca N, Lambolez B, Rossier J, Hamel E (2004) Cortical GABA interneurons in neurovascular coupling: relays for subcortical vasoactive pathways. J Neurosci 24:8940–8949

Chaimow D, Yacoub E, Uğurbil K, Shmuel A (2015) Spatial specificity of the functional MRI blood oxygenation response relative to metabolic activity. Annual meting of the Society for Neuroscience. Chicago, USA

Cohen LB, De Weer P (1977) Structural and metabolic processes directly related to action potential propagation. In: Brookhart JM, Mountcastle VB (eds) Handbook of physiology: the nervous system. American Physiological Society, Bethesda, pp 137–159

DeFelipe J, Alonso-Nanclares L, Arellano JI (2002) Microstructure of the neocortex: comparative aspects. J Neurocytol 31:299–316

Devor A, Dunn AK, Andermann ML, Ulbert I, Boas DA, Dale AM (2003) Coupling of total hemoglobin concentration, oxygenation, and neural activity in rat somatosensory cortex. Neuron 39:353–359

Devor A, Tian P, Nishimura N, Teng IC, Hillman EMC, Narayanan SN, Ulbert I, Boas DA, Kleinfeld D, Dale AM (2007) Suppressed neuronal activity and concurrent arteriolar vasoconstriction may explain negative blood oxygenation level-dependent signal. J Neurosci 27:4452–4459

Douglas RJ, Martin KAC (2004) Neuronal circuits of the neocortex. Annu Rev Neurosci 27:419–451

Douglas RJ, Martin KAC, Whitteridge D (1989) A canonical microcircuit for neocortex. Neural Comput 1:480–488

Engel SA, Glover GH, Wandell BA (1997) Retinotopic organization in human visual cortex and the spatial precision of functional MRI. Cereb Cortex 7:181–192

Felleman DJ, Van Essen, DC (1991) Distributed hierarchical processing in the primate cerebral cortex. Cereb Cortex 1:1–47

Fox PT, Raichle ME (1986) Focal physiological uncoupling of cerebral blood-flow and oxidative-metabolism during somatosensory stimulation in human-subjects. Proc Natl Acad Sci U S A 83:1140–1144

Fox MD, Raichle ME (2007) Spontaneous fluctuations in brain activity observed with functional magnetic resonance imaging. Nat Rev Neurosci 8(9):700–711

Freeman, WJ (1975) Mass action in the nervous system. Academic, New York

Goense JBM, Logothetis NK (2008) Neurophysiology of the BOLD fMRI Signal in Awake Monkeys. Curr Biol 18:631–640

Hamel E (2004) Cholinergic modulation of the cortical microvascular bed. Prog Brain Res 145:171–178

Handwerker DA, Bandettini PA (2011) Hemodynamic signals not predicted? Not so: a comment on Sirotin and Das (2009). Neuroimage 55(4):1409–1412

Hansen BJ, Dragoi V (2011) Adaptation-induced synchronization in laminar cortical circuits. Proc Natl Acad Sci U S A 108:10720–10725

Harel N, Lee SP, Nagaoka T, Kim DS, Kim SG (2002) Origin of negative blood oxygenation level-dependent fMRI signals. J Cereb Blood Flow Metab 22:908–917
Haug H (1987) Brain sizes, surfaces, and neuronal sizes of the cortex cerebri: a stereological investigation of man and his variability and a comparison with some mammals (primates, whales, marsupials, insectivores, and one elephant). Am J Anat 180:126–142
Heeger DJ, Huk AC, Geisler WS, Albrecht DG (2000) Spikes versus BOLD: what does neuroimaging tell us about neuronal activity? Nat Neurosci 3:631–633
Hoffmeyer HW, Enager P, Thomsen KJ, Lauritzen MJ (2007) Nonlinear neurovascular coupling in rat sensory cortex by activation of transcallosal fibers. J Cereb Blood Flow Metab 27:575–587
Hoge RD, Atkinson J, Gill B, Crelier GR, Marrett S, Pike GB (1999) Linear coupling between cerebral blood flow and oxygen consumption in activated human cortex. Proc Natl Acad Sci U S A 96:9403–9408
Horton JC, Adams DL (2005) The cortical column: a structure without a function. Philos Trans R Soc Lond B Biol Sci 360:837–862
Hubel DH, Wiesel TN (1974) Uniformity of monkey striate cortex: a parallel relationship between field size, scatter, and magnification factor. J Comp Neurol 158:295–305
Jones M, Hewson-Stoate N, Martindale J, Redgrave P, Mayhew J (2004) Nonlinear coupling of neural activity and CBF in rodent barrel cortex. Neuroimage 22:956–965
Juergens E, Guettler A, Eckhorn R (1999) Visual stimulation elicits locked and induced gamma oscillations in monkey intracortical- and EEG-potentials, but not in human EEG. Exp Brain Res 129:247–259.
Kannurpatti SS, Biswal BB (2004) Negative functional response to sensory stimulation and its origins. J Cereb Blood Flow Metab 24:703–712
Kwong KK, Belliveau JW, Chesler DA, Goldberg IE, Weisskoff RM, Poncelet BP, Kennedy DN, Hoppel BE, Cohen MS, Turner R, Cheng HM, Brady TJ, Rosen BR (1992) Dynamic magnetic resonance imaging of human brain activity during primary sensory stimulation. Proc Natl Acad Sci U S A 89:5675–5679
Lauritzen M (2005) Reading vascular changes in brain imaging: is dendritic calcium the key? Nat Rev Neurosci 6:77–85
Leopold DA, Murayama Y, Logothetis NK (2003) Very slow activity fluctuations in monkey visual cortex: implications for functional brain imaging. Cereb Cortex 13:423–433
Logothetis NK (2002) The neural basis of the blood-oxygen-level-dependent functional magnetic resonance imaging signal. Phil Trans R Soc Lond B 357:1003–1037
Logothetis NK (2010) Neurovascular uncoupling: much ado about nothing. Front Neuroenerg 2:2
Logothetis NK, Pauls J, Augath M, Trinath T, Oeltermann A (2001) Neurophysiological investigation of the basis of the fMRI signal. Nature 412:150–157
Lübke J, Feldmeyer D (2007) Excitatory signal flow and connectivity in a cortical column: focus on barrel cortex. Brain Struct Funct 212:3–17
Maier A, Wilke M, Aura C, Zhu C, Ye FQ, Leopold DA (2008) Divergence of fMRI and neural signals in V1 during perceptual suppression in the awake monkey. Nat Neurosci 11(10):1193–1200
Maier A, Adams GK, Aura C, Leopold DA (2010) Distinct superficial and deep laminar domains of activity in the visual cortex during rest and stimulation. Front Syst Neurosci 4:31. doi:10.3389/fnsys.2010.00031
Maier A, Aura CJ, Leopold DA (2011) Infragranular sources of sustained local field potential responses in macaque primary visual cortex. J Neurosci 31:1971–1980
Marín-Padilla M (1998) Cajal-Retzius cells and the development of the neocortex. Trends Neurosci 21:64–71
Mathiesen C, Caesar K, Akgoren N, Lauritzen M (1998) Modification of activity dependent increases of cerebral blood flow by excitatory synaptic activity and spikes in rat cerebellar cortex. J Physiol (Lond) 512:555–566
Maunsell JH, Gibson JR (1992) Visual response latencies in striate cortex of the macaque monkey. J Neurophysiol 68:1332–1344

Mayhew JE, Askew S, Zheng Y, Porrill J, Westby GW, Redgrave P, Rector DM, Harper RM (1996) Cerebral vasomotion: a 0.1-Hz oscillation in reflected light imaging of neural activity. Neuroimage 4:183–193

Mittmann W, Wallace DJ, Czubayko U, Herb JT, Schaefer AT, Looger LL, Denk W, Kerr JND (2011) Two-photon calcium imaging of evoked activity from L5 somatosensory neurons in vivo. Nat Neurosci 14:1089–1093

Mitzdorf U (1987) Properties of the evoked potential generators: current source-density analysis of visually evoked potentials in the cat cortex. Int J Neurosci 33:33–59.

Mukamel R, Gelbard H, Arieli A, Hasson U, Fried I, Malach R (2005) Coupling between neuronal firing, field potentials, and fMR1 in human auditory cortex. Science 309:951–954

Nelson S (2002) Cortical microcircuits: diverse or canonical? Neuron 36:19–27

Nicholson, C (1973) Theoretical analysis of field potentials in anisotropic ensembles of neuronal elements. IEEE Trans Biomed Eng 20:278–288

Nielsen A, Lauritzen M (2001) Coupling and uncoupling of activity-dependent increases of neuronal activity and blood flow in rat somatosensory cortex. J Physiol (Lond) 533:773–785

Niessing J, Ebisch B, Schmidt KE, Niessing M, Singer W, Galuske RA (2005) Hemodynamic signals correlate tightly with synchronized gamma oscillations. Science 309:948–951

Nir Y, Fisch L, Mukamel R, Gelbard-Sagiv H, Arieli A, Fried I, Malach R (2007) Coupling between neuronal firing rate, gamma LFP, and BOLD fMRI is related to interneuronal correlations. Curr Biol 17:1275–1285

Nowak LG, Munk MH, Girard P, Bullier J (1995) Visual latencies in areas V1 and V2 of the macaque monkey. Vis Neurosci 12:371–384

Ogawa S, Lee TM, Kay AR, Tank DW (1990) Brain magnetic resonance imaging with contrast dependent on blood oxygenation. Proc Natl Acad Sci U S A 87:9868–9872

Ogawa S, Tank DW, Menon R, Ellermann JM, Kim SG, Merkle H, Uğurbil K (1992) Intrinsic signal changes accompanying sensory stimulation: functional brain mapping with magnetic-resonance-imaging. Proc Natl Acad Sci U S A 89:5951–5955

Pasley BN, Inglis BA, Freeman RD (2007) Analysis of oxygen metabolism implies a neural origin for the negative BOLD response in human visual cortex. Neuroimage 36:269–276

Pedemonte M, Barrenechea C, Nunez A, Gambini, JP, Garcia-Austt E (1998) Membrane and circuit properties of lateral septum neurons: relationships with hippocampal rhythms. Brain Res 800:145–153

Peters A, Payne BR (1993) Numerical relationships between geniculocortical afferents and pyramidal cell modules in cat primary visual cortex. Cereb Cortex 3:69–78

Peters A, Sethares CJ (1991) Organization of pyramidal neurons in area 17 of monkey visual cortex. J Comp Neurol 306:1–23

Polimeni JR, Fischl B, Greve DN, Wald LL (2010) Laminar analysis of 7T BOLD using an imposed spatial activation pattern in human V1. NeuroImage 52:1334–1346

Raichle ME, Mintum MA (2006) Brain work and brain imaging. Annu Rev Neurosci 29:449–476

Rauch A, Rainer G, Logothetis NK (2008) The effect of a serotonin-induced dissociation between spiking and perisynaptic activity on BOLD functional MRI. Proc Natl Acad Sci U S A 105:6759–6764

Rees G, Friston K, Koch C (2000) A direct quantitative relationship between the functional properties of human and macaque V5. Nat Neurosci 3:716–723

Ritchie JM (1967) The oxygen consumption of mammalian non-myelinated nerve fibers at rest and during activity. J Physiol (Lond) 188:309–329

Rockel AJ, Hiorns RW, Powell TP (1980) The basic uniformity in structure of the neocortex. Brain 103:221–244

Saad ZS, Ropella KM, DeYoe EA, Bandettini PA (2003) The spatial extent of the BOLD response. Neuroimage 19:132–144

Schölvinck M, Maier A, Ye F, Duyn, J, Leopold DA (2010) Neural basis of global resting-state fMRI activity. Proc Natl Acad Sci U S A 107(22):10238–10243

Schroeder CE, Mehta AD, Givre SJ (1998) A spatiotemporal profile of visual system activation revealed by current source density analysis in the awake macaque. Cereb Cortex 8:575–592

Schwartz WJ, Smith CB, Davidsen L, Savaki H, Sokoloff L, et al (1979) Metabolic mapping of functional activity in the hypothalamo-neurohypophysial system of the rat. Science 205:723–725

Sheth SA, Nemoto M, Guiou M, Walker M, Pouratian N, Toga AW (2004) Linear and nonlinear relationships between neuronal activity, oxygen metabolism, and hemodynamic responses. Neuron 42:347–355

Shmuel A, Grinvald A (1996) Functional organization for direction of motion and its relationship to orientation maps in cat area 18. J Neurosci 16:6945–6964, and cover illustration

Shmuel A, Leopold DA (2008) Neuronal correlates of spontaneous fluctuations in fMRI signals in monkey visual cortex: implications for functional connectivity at rest. Hum Brain Mapp 29:751–761

Shmuel A, Yacoub E, Pfeuffer J, Van de Moortele PF, Adriany G, Hu XP, Uğurbil K (2002) Sustained negative BOLD, blood flow and oxygen consumption response and its coupling to the positive response in the human brain. Neuron 36:1195–1210

Shmuel A, Augath M, Oeltermann A, Logothetis NK (2006) Negative functional MRI response correlates with decreases in neuronal activity in monkey visual area V1. Nat Neurosci 9:569–577

Shmuel A, Yacoub E, Chaimow D, Logothetis NK, Uğurbil K (2007), Spatio-temporal point-spread function of fMRI signal in human gray matter at 7 Tesla. Neuroimage 35:539–552

Sirotin YB, Das A (2009) Anticipatory haemodynamic signals in sensory cortex not predicted by local neuronal activity. Nature 457(7228):475–479.

Smith AJ, Blumenfeld H, Behar KL, Rothman DL, Shulman RG, Hyder F (2002) Cerebral energetics and spiking frequency: the neurophysiological basis of fMRI. Proc Natl Acad Sci U S A 99:10765–10770

Snodderly DM, Gur M (1995) Organization of striate cortex of alert, trained monkeys (*Macaca fascicularis*): ongoing activity, stimulus selectivity, and widths of receptive field activating regions. J Neurophys 74:2100–2125

Sokoloff L, Reivich M, Kennedy C, Des Rosiers MH, Patlak CS, Pettigrew KD, Sakurada O, Shinohara M (1977) The [14C] deoxyglucose method for the measurement of local glucose utilization: theory, procedure and normal values in the conscious and anesthetized albino rat. J Neurochem 28:897–916

Sotero RC, Bortel A, Martínez-Cancino R, Neupane S, O'Connor P, Carbonell F, Shmuel A (2010) Anatomically-constrained effective connectivity among layers in a cortical column modeled and estimated from local field potentials. J Integr Neurosci 9:355–379

Stefanovic B, Warnking JM, Pike GB (2004) Hemodynamic and metabolic responses to neuronal inhibition. Neuroimage 22:771–778

Stefanovic B, Warnking JM, Kobayashi E, Bagshaw AP, Hawco C, Dubeau F, Gotman J, Pike GB (2005) Hemodynamic and metabolic responses to activation, deactivation and epileptic discharges. Neuroimage 28:205–215

Tan CA (2009) Anticipatory changes in regional cerebral hemodynamics: a new role for dopamine? J Neurophysiol 101:2738–2740

Thomsen K, Offenhauser N, Lauritzen M (2004) Principle neuron spiking: neither necessary nor sufficient for cerebral blood flow at rest or during activation in rat cerebellum. J Physiol (Lond) 560:181–189

Thomson AM, Bannister AP (2003) Interlaminar connections in the neocortex. Cereb Cortex (New York, NY: 1991) 13:5–14

Uludağ K, Dubowitz DJ, Yoder EJ, Restom K, Liu TT, Buxton RB (2004) Coupling of cerebral blood flow and oxygen consumption during physiological activation and deactivation measured with fMRI. Neuroimage 23:148–155

Viswanathan A, Freeman RD (2007) Neurometabolic coupling in cerebral cortex reflects synaptic more than spiking activity. Nat Neurosci 10:1308–1312

Wise RJS, Ide K, Poulin MJ, Tracey I (2004) Resting state fluctuations in arterial carbon dioxide induce significant low frequency variations in BOLD signal. Neuroimage 21:1652–1664